Available online at www.sciencedirect.com

SciVerse ScienceDirect

Physics Procedia 36 (2012) 638 – 643

Physics Procedia

Superconductivity Centennial Conference

Single crystal growth and transport properties of Cu-doped topological insulator Bi_2Se_3

Z.J. Li[a,b], Y. Liu[a], S.C. White[a], P. Wahl[a], X.M. Xie[b], M.H. Jiang[b], and C.T. Lin[a*]

[a]*Max Planck Institute for Solid State Research, Heisenbergstaße 1, D-70569 Stuttgart, Germany*

[b]*Shanghai Institute of Microsystem and Information Technology, Changning Road 865, 200050 Shanghai, China*

Abstract

We report on the growth of high quality single crystals of $Cu_xBi_2Se_3$ with x=0, 0.12 and 0.15, using Bridgman method. A study of crystal structure shows that the *c*-lattice parameter slightly decreases with an increasing level of Cu-doping. STM images indicate that both Cu-intercalation between Se-Se layers and Cu-substitution in Bi-layer sites are present. With dc magnetization measurements, superconducting transitions in Cu-intercalated Bi_2Se_3 have been found with a T_C of 3.5 K for x~0.12 and approximately 3.6 K for x~0.15, respectively. The resistivity data show metallic behavior in the Bi_2Se_3 crystals and paramagnetic features are observed in the low temperature region of the Cu-doped samples.

Keywords: Bi_2Se_3; Topological insulators; Superconductivity

1. Introduction

Topological insulators (TIs) are a novel kind of material which appears to be insulating in the bulk while conducting on the surface. Notably, the gapless surface state is robust and topologically protected against disorder by time-reversal symmetry. As a result, electrons experience no back-scattering by nonmagnetic impurities [1-6]. Several materials have been predicted to be TIs and were subsequently shown experimentally to exhibit TI behaviors, such as Bi_xSb_{1-x} alloys [7], Bi_2Se_3, Bi_2Te_3, Sb_2Te_3 crystals [8-9], and Heusler compounds [10]. In one such material, Bi_2Se_3, which is well known for its good thermoelectric properties [11], the effects of chemical doping on structure, transport and magnetic properties have been widely studied. It is notable that the topological insulator Bi_2Se_3, through

* Corresponding author.
E-mail address: ct.lin@fkf.mpg.de

1875-3892 doi:10.1016/j.phpro.2012.06.182

intercalation of Cu between Se-Se layers, can be turned into a superconductor with a transition temperature of up to 3.8 K [12-13]. It may therefore be possible to create an interface between a topological insulator and a topological superconductor, which would be useful for a detailed investigation into some of the intriguing phenomena of the topological insulators. Here we report on the transport and magnetic properties of Cu-doped topological insulator Bi_2Se_3 for both the substitution and intercalation cases.

2. Experiment

Single crystals of $Cu_xBi_2Se_3$ with nominal x values of 0, 0.12 and 0.15 were grown from stoichiometric mixtures of high purity (5N) Bi, Se and Cu powders. All preparation procedures were carried out in a glove box under argon atmosphere. The powders were first weighed and loaded into quartz ampoules. The ampoules were then evacuated, sealed and loaded into a vertical furnace. For pure Bi_2Se_3, the ampoule was heated up to 750 ˚C, followed by a 12 h soaked, and then slowly cooled to 650 ˚C at 3 ˚C/h. Thereafter, the crystal was allowed to furnace-cool down to room temperature. For Cu-doped Bi_2Se_3, the mixtures were melted at 850˚C for 12h, then slowly cooled to 620 ˚C at 3˚C/h and subsequently quenched in cold water. The obtained crystals were ϕ6 x 40-50 mm. As-grown crystals exhibited a metallic appearance on the surface and were easily cleavable due to their layered structure. Crystal compositions were determined by energy dispersive x-ray spectroscopy (EDX). X-ray diffraction (XRD) analysis, using Bruker D8 with Cu K_α radiation, was performed to identify the phase purity and the crystal structure. Resistivity measurements were carried out with a physical property measurement system (PPMS™, Quantum Design). The magnetic properties were obtained using a SQUID (VSM, Quantum Design) magnetometer. A cryogenic scanning tunneling microscope was used for topographical characterization.

3. Results and discussion

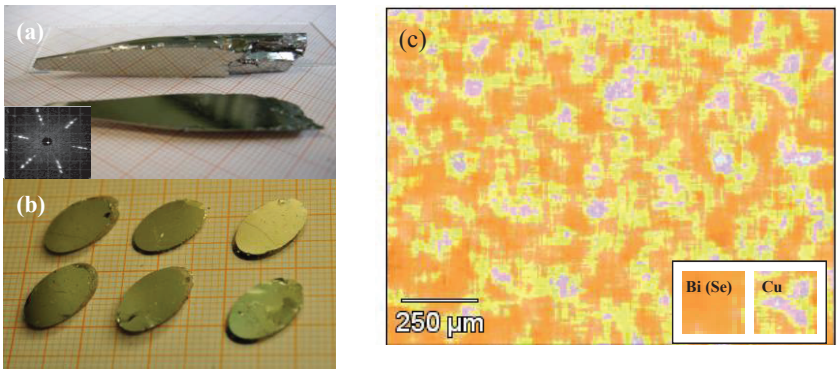

Fig. 1 As-grown single crystals of $Cu_xBi_2Se_3$ (a) x~0.12 showing crown cylinder shape formed in ampoule and naturally cleaved *(00l)* face; (b) the *(00l)* wafers with x~0.15; (c) EDX mapping shows the distribution of Bi/ Se (orange color), Cu (pink color) three elements in the $Cu_{0.15}Bi_2Se_3$ single crystal.

As-grown pure and Cu-doped Bi_2Se_3 single crystals exhibit a shiny and metallic surface. The morphology of the crystals is formed with crown cylinder like ampoule shape, as shown in Fig. 1(a). The cleavable face exhibits the *(001)* crystallographic plane due to the layered structure along the *c* direction. The inset of Fig. 1(a) is the clean *(00l)* Laue patterns showing the six symmetric structure. Fig. 1(b) shows the *(00l)* wafers readily cleaved from the crystal cylinder. The micrograph of EDX mapping

demonstrates distribution of Cu with atomic ratio approximately 15% in the sample as shown in fig. 1(c). Fig. 2(a) is the *(00l)* XRD patterns obtained on the naturally cleaved surface, indicating a good crystallization along the *c* axis of the crystals. The powder XRD patterns in Fig. 2(b) can be well indexed within the space group R-3m (166). All the samples are single phase and belong to the rhombohedral layered structure group typical of Bi_2Se_3 [11]. The lattice parameters for both *a* and *c* were estimated to slightly decrease with increasing Cu doping content. The results are summarized in Table 1. Fig. 2(c) shows a nearly linear relationship between the Cu doping level and the *c*-parameters. It has been reported that there are two ways for Cu atoms to enter the Bi_2Se_3 crystal lattice. The Cu atoms are either incorporated into the lattice at Bi-sites to form a substitutional solid solution or are intercalated between Se-Se layers [14]. The former possibility leads to a decreasing of lattice constants for both the *a* and *c* axes due to the fact that the Cu^{2+} ion radius (0.72 Å) is smaller than that of Bi^{3+} (1.08 Å). Compared to the former case, in the case of intercalation between Se-Se layers there should be a significant increase in the *c*-axis lattice constant [12]. Therefore, the observed development of the lattice constants in our Cu-doped Bi_2Se_3 samples should mostly be attributed to Cu-substitution at Bi-sites.

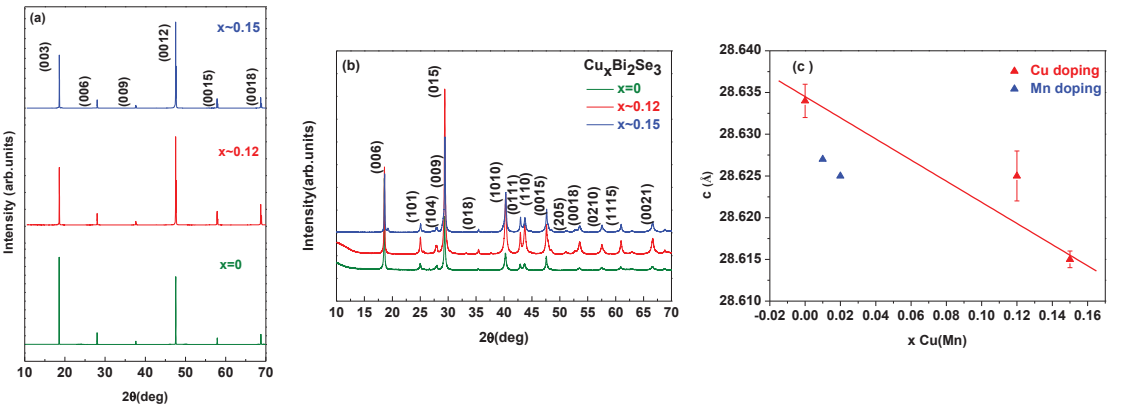

Fig. 2 XRD patterns showing (a) the (00l) reflections on the natural cleaved surface and (b) powder crystal XRD patterns for the pure and CuxBi2Se3. (c) the line is guided to eye, showing the c-parameters decreasing with Cu-doping level in Bi2Se3. The blue points are from Mn doping referred with ref. [16].

Table 1. The lattice parameters of pure and Cu-doped Bi_2Se_3

Nominal composition	a (Å)	c(Å)	c/a	V(Å^3)
Bi_2Se_3	4.1396(8)	28.634(2)	6.917	424.93
$Cu_{0.12}Bi_2Se_3$	4.1357(6)	28.625(3)	6.921	424.02
$Cu_{0.15}Bi_2Se_3$	4.1349(3)	28.615(1)	6.920	423.69

The temperature dependence of resistivity in the *ab*-plane for pure and Cu-substituted Bi_2Se_3 is shown in Fig. 3(a), which indicates a typical metallic behavior. None of the curves showed a transition to superconductivity down to ~2 K, which is the lowest temperature our apparatus can achieve. Bi_2Se_3 does not show the expected insulating behavior due to the Se vacancies in the lattice [15]. Compared to pure

Bi_2Se_3, the addition of Cu leads to a strong decrease in the resistivity. Meanwhile, magnetoresistance effect is observed in the sample $Cu_{0.15}Bi_2Se_3$, as shown in inset of Fig. 3(a). By applying a magnetic field of 1kOe, the resistivity exhibits semiconductor behavior. Further study and discussion on this phenomenon is required.

Fig. 3(b) shows temperature-dependent magnetic susceptibility curves of pure and Cu-substituted Bi_2Se_3. The measurements were performed in zero-field-cooled mode under 10 kOe. Our measurements show Bi_2Se_3 to be diamagnetic with a temperature-independent susceptibility of $2x10^{-6}$. The magnetization curves of Cu-substituted Bi_2Se_3 show paramagnetic behavior at low temperature. With increasing temperature, a strong diamagnetic contribution from the Bi_2Se_3 host can be seen in Fig. 3(b).

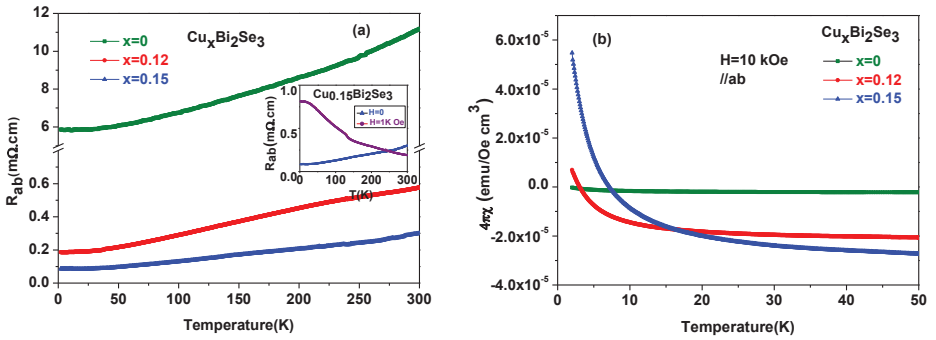

Fig. 3 (a) Temperature dependence of resistivity and (b) magnetic susceptibility for pure and Cu-substituted Bi_2Se_3, measured in a magnetic field of 10 kOe. Inset is the temperature dependence of resistivity for $Cu_{0.15}Bi_2Se_3$ measured under 1 kOe magnetic field.

The effects of intercalated Cu between the Se-Se layers are confirmed by dc magnetization measurements under 10 Oe in zero-field-cooled mode. The results are shown in Figs. 4(a) and (b) respectively. A clear diamagnetic signal is observed at T_c=3.5 K for $Cu_{0.12}Bi_2Se_3$. The superconducting transition occurs at T_c=3.6 K for $Cu_{0.15}Bi_2Se_3$. It is noted that these superconducting samples were selected from the tail part of the crystals, while the other part shows no superconductivity due to a slight variation of the crystal composition.

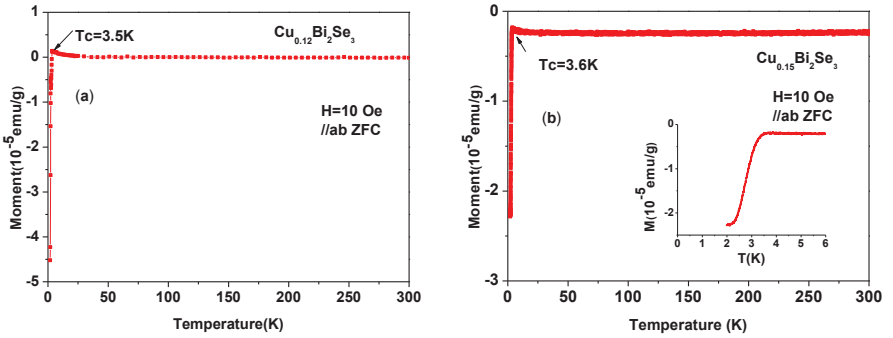

Fig. 4 Temperature dependence of magnetic susceptibility for (a) $Cu_{0.12}Bi_2Se_3$; (b) $Cu_{0.15}Bi_2Se_3$, Inset gives an enlargement around the superconducting transition.

The $Cu_{0.12}Bi_2Se_3$ sample with nominal composition was confirmed to be superconducting by SQUID measurements and then measured in an STM. The images in Figs. 5(a) and (b) were taken at 4.2 K, with 0.8 nA and 0.1 V. Along with a hexagonal pattern of surface Se atoms, several types of surface and subsurface impurities are visible, for instance small tri-atomic depressions, larger elevated areas with a triangular form, and clusters on the surface. We believe the elevated triangular areas to be associated with atomic Cu intercalated between the van der Waals bonded layers. Based on the STM images, we conclude that both Cu intercalated between Se-Se layers and Cu occupying Bi-sites are present in the examined crystal.

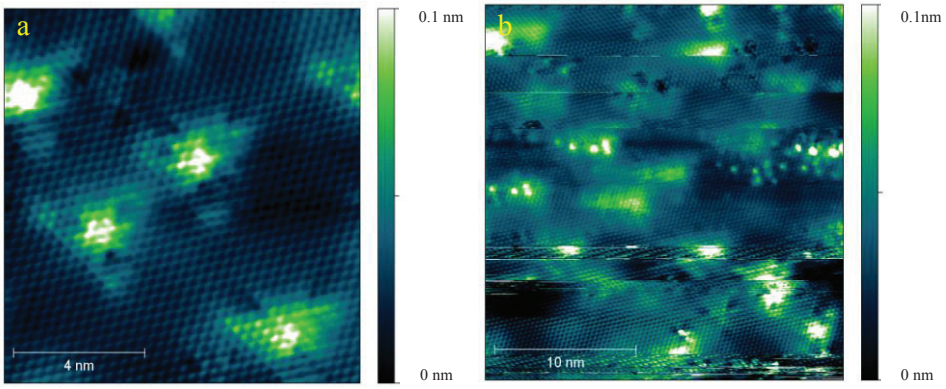

Fig. 5 STM topography (0.8 nA, 0.1 V) of $Cu_{0.12}Bi_2Se_3$ over (a) 10 nm by 10nm (b) 25 nm by 25 nm area, showing an atomically resolved hexagonal pattern of Se and several types of defects.

4. Conclusion

Pure and Cu-doped Bi_2Se_3 bulk single crystals were grown with a modified Bridgman method. Both Cu-substitution and Cu-intercalation are observed in our samples. The decrease in the size of both the lattice parameters and the unit-cell volume with increasing Cu doping indicates that Cu atoms mostly substitute for Bi within the host structure. Compared to the parent phase Bi_2Se_3, a decrease in resistivity for Cu-substituted samples is observed. The parent compound Bi_2Se_3 exhibits temperature-independent diamagnetism. With doping via Cu-substitution, the samples begin to show weak paramagnetic behavior at low temperatures. Superconductivity is measured in Cu-intercalated Bi_2Se_3 with a T_C of 3.5 K for x~0.12 and 3.6 K with x~0.15, respectively.

Acknowledgements

We thank C. Stefani for the XRD measurements, C. Busch for the analysis of crystal composition, and H. Bender for technical support.

References

[1] L. Fu, C. L. Kane, E. J. Mele, Phys. Rev. Lett. **98**, 106803 (2007).
[2] J. Moore, Nature Phys. **5**, 378 (2009).
[3] X. L. Qi, S. C. Zhang, Physics Today, 33 January 2010.
[4] J. Moore, Nature. **464**, 194 (2010).
[5] M. Z. Hasan, J. Moore, arXiv: 1011.5462v1, (2010).
[6] M. Z. Hasan, C. L. Kane, Rev. Mod. Phys. **82**, 3045 (2010).
[7] D. Hsieh, D. Qian, L, Wray, Y. Xia, Y. S. Hor, R. J. Cava et al., Nature. **452**, 970 (2008).
[8] H. J. Zhang, C. X. Liu, X. L. Qi, X. Dai, Z. Fang, S. C. Zhang, Nature Physics **5**, 438 (2009).
[9] Y. Xia, D. Qian, D. Hsieh, L. Wray, A. Pal, H. Lin et al, Nature Physics **5**, 398 (2009).
[10] M. Franz, Nature Materials **9**, 536 (2010)
[11] H. Scherrer, S. Scherrer, in: D.M. Rowe (Ed.), CRC Handbook of Thermoelectrics, Chemical Rubber, Boca Raton, FL1995, pp. 211–237
[12] Y. S. Hor, A. J. Williams, J. G. Checkelsky, P, Poushan, J. Seo, Q. Xu et al, Phys. Rev. Lett. **104**, 057001 (2010)
[13] Y. S. Hor, J. G. Checkelsky, D. Xu, N. P. Ong, R. J. Cava, J. Phys. Chem. Solids. **72**, 572 (2010)
[14] A. Vásko, L. Tichý, J. Horák, J. Weissenstein, Appl. Phys. **5**, 217 (1974).
[15] Ĉ. Drašar, I. Klichová, L. Koudelka, P. Lošťák, Cryst. Res. Technol. **31,** 805 (1996).
[16] P. Janíček, Ĉ. Drašar, P. Lošťák, J. vejpravová, V. Sechovský, Physica B **403**. 3553 (2008)